

1 **Title: Genetic (in)stability of 2,6-dichlorobenzamide (BAM)-catabolism in *Aminobacter* sp.**
2 **MSH1 biofilms under carbon starved conditions**

3 Running title: Catabolic (in)stability in carbon starved bacterial biofilms

4 Authors: Benjamin Horemans^{1,*}, Bart Raes¹, Hannelore Brocatus¹, Jeroen T'Syen¹, Caroline
5 Rombouts², Lynn Vanhaecke², Johan Hofkens³, Dirk Springael¹

6 Affiliations:

7 ¹ Division of Soil and Water Management, Department of Earth and Environmental Sciences, Faculty
8 of Bioscience Engineering, KU Leuven, Kasteelpark Arenberg 20 bus 2459, 3001 Heverlee, Belgium

9 ² Faculty of Veterinary Medicine, Department of Veterinary Public Health and Food Safety,
10 Laboratory of Chemical Analysis, UGent, Salisburylaan 133, 9820 Merelbeke, Belgium

11 ³ Molecular Imaging and Photonics, KU Leuven, 3001 Leuven, Belgium

12
13 * Corresponding author: benjamin.horemans@kuleuven.be

14 Dr. Ir. Benjamin Horemans

15 Division of Soil and Water Management, KU Leuven, Kasteelpark Arenberg 20, 3001 Heverlee,
16 Belgium.

17 Phone: +32(0)16329675; fax: +32(0)16321997

18 e-mail: Benjamin.horemans@kuleuven.be

19

20 Keywords: 2,6-dichlorobenzamide, catabolic instability, micropollutant, starvation conditions

21 **Abstract**

22 *Aminobacter* sp. MSH1 grows on and mineralizes the groundwater micropollutant 2,6-
23 dichlorobenzamide (BAM) and is of interest for BAM removal in drinking water treatment
24 plants (DWTPs). The BAM-catabolic genes in MSH1 are located on plasmid pBAM1 carrying
25 *bbdA* encoding the conversion of BAM to 2,6-dichlorobenzoic acid (2,6-DCBA) (*BbdA*⁺
26 phenotype) and plasmid pBAM2 carrying gene clusters encoding the conversion of 2,6-DCBA
27 to TCA cycle intermediates (*Dcba*⁺ phenotype). Indications exist that MSH1 loses easily its
28 BAM-catabolic phenotype. Evidence was obtained that MSH1 rapidly develops a population
29 that lacks the ability to mineralize BAM when grown on non-selective (R2B medium) and
30 semi-selective (R2B with BAM) medium. Lack of mineralization was explained by loss of the
31 *Dcba*⁺ phenotype and corresponding genes. The ecological significance of this instability for
32 the use of MSH1 for BAM removal in the oligotrophic environment of DWTPs was explored
33 in lab and pilot systems. A higher incidence of *BbdA*⁺ *Dcba*⁻ MSH1 cells was also observed
34 when MSH1 was grown as biofilms in flow chambers under C and N starved conditions due
35 to growth on non-selective residual assimilable organic carbon. Similar observations were
36 done in a pilot sand filter reactor bioaugmented with MSH1. BAM conversion to 2,6-DCBA
37 was though not affected by loss of the DCBA catabolic genes. Our results show that MSH1 is
38 prone to BAM-catabolic instability under the conditions occurring in a DWTP. While
39 conversion of BAM to 2,6-DCBA remains unaffected, BAM-mineralization activity is at risk
40 and monitoring of metabolites is warranted.

41 **Importance**

42 Bioaugmentation of dedicated biofiltration units in DWTPs with bacterial strains that grow
43 on and mineralize micropollutants was suggested as an alternative for treating
44 micropollutant-contaminated water in a drinking water treatment plant (DWTP). Organic
45 pollutant catabolic genes in bacteria are often easily lost especially under non-selective
46 conditions which will affect the bioaugmentation success. In this study, we provide evidence
47 that *Aminobacter* sp. MSH1 that uses the common groundwater micropollutant 2,6-
48 dichlorobenzamide (BAM) as a C-source, shows a high frequency of loss of its BAM-
49 mineralizing phenotype due the loss of genes that convert 2,6-DCBA to Krebs cycle
50 intermediates when non-selective conditions occur. Moreover, we show that catabolic gene
51 loss also occurs in the oligotrophic environment of DWTPs where growth of MSH1 mainly
52 depends on the high fluxes of low concentration of assimilable organic carbon and hence
53 show the ecological relevance of catabolic instability for using strain MSH1 for BAM removal
54 in DWTPs.

55 Introduction

56 2,6-dichlorobenzamide (BAM), a transformation product of the herbicide dichlobenil, is a
57 major groundwater micropollutant that hampers groundwater-based drinking water
58 production. Concentrations of BAM in groundwater are typically in the trace concentration
59 range of ng- μ g/L (1, 2), frequently surpassing the EU threshold limit of 0.1 μ g/L for drinking
60 water (3). Wells that extract BAM-contaminated groundwater intended for drinking water
61 production are either closed or drinking water treatment plants (DWTPs) (4) employ
62 additional expensive treatment steps such as granular activated carbon (GAC) filtration or
63 ozonization to lower the BAM concentration below the EU threshold limit (5, 6).
64 Bioremediation is suggested as a green and economically sound alternative to remove
65 micropollutants from water intended for drinking water consumption in DWTPs (7, 8).
66 *Aminobacter* sp. MSH1 is an aerobic soil isolate that mineralizes BAM and uses the
67 compound as C, N and energy source (2, 9). The organism was proposed as a candidate
68 biological catalysts for bioaugmentation of dedicated filtration units in DWTPs to treat BAM
69 contaminated intake water (8).

70 Bioaugmentation in DWTPs for the treatment of micropollutants is, however, challenging
71 since the inoculated strain needs to maintain sufficient biomass and pollutant degrading
72 activity in the highly oligotrophic conditions (7). In a recent study, strain MSH1 was grown as
73 biofilms in flow channels continuously fed with mineral salts medium containing BAM
74 concentrations as low as 1 μ g/L BAM (10). Below feed concentrations of 100 μ g/L BAM,
75 growth of MSH1 is mainly due to residual assimilable organic carbon (AOC) present in the
76 minimal medium. Moreover, MSH1 specific BAM-degrading activity was reduced 100-fold
77 compared to freshly grown cells due to C and/or N starvation (10). A similar reduction in

78 specific BAM-degrading activity was found in a DWTP pilot scale sand filter study that
79 investigated bioaugmentation with *Aminobacter* sp. MSH1 for treating BAM-contaminated
80 groundwater (9). An often observed feature of organic xenobiotic degrading bacteria, that
81 might contribute to reduced activity, is instability of the genes encoding pollutant
82 catabolism. The genes encoding catabolic pathways for organic xenobiotic degradation are
83 often located on plasmids and/or bordered by insertion elements at both sites of the
84 catabolic cluster. Segregation of a catabolic strain into variants that lost the catabolic
85 phenotype when the strain is grown on (specified) non-selective conditions, was observed in
86 various xenobiotic catabolic strains due to either complete plasmid loss or intramolecular
87 genetic rearrangements (11). The genes that encode BAM metabolism and hence BAM-
88 mineralization in MSH1 are carried by two plasmids, i.e., the IncP-1 plasmid pBAM1 that
89 contains the *bbdA* gene responsible for conversion of BAM to 2,6-dichlorobenzoic acid (2,6-
90 DCBA) (*BbdA*⁺ phenotype) (12) and the *repABC* family plasmid pBAM2 that carries two gene
91 clusters responsible for degradation of 2,6-DCBA to Krebs cycle intermediates (*Dcba*⁺
92 phenotype), i.e., *bbdR1B1B2B3CDE* and *bbdFGHIJK* (T'Syen, unpublished results). Mutants
93 that lack one of the two or both genotypes and hence are defective in BAM-mineralization,
94 were isolated when MSH1 was grown on non-selective medium indicating that the strain is
95 genetically unstable regarding BAM-mineralization and catabolism (12).

96 The micropollutant concentrations of BAM present in DWTP intake water represents only a
97 minority of the organic carbon available for growth. Instead, as reported above, growth of
98 MSH1 will mainly depend on the high fluxes of low concentrations of AOC in the water which
99 will impose non-selective conditions for MSH1 and his BAM-catabolic features. This might
100 result into the loss of the BAM-catabolic genes which likely affects BAM-degrading activity.

101 In this study, we examined conditions under which a MSH1 population loses the BAM-
102 catabolic phenotype and determined whether this might also occur and affect BAM-
103 degradation activity in MSH1 biofilms grown under the C and N starved conditions that occur
104 in DWTPs.

105 **Material and methods**

106 **Media preparation and bacterial cultivation.** *Aminobacter* sp. MSH1-GFP, a green
107 fluorescent protein (GFP) labeled and kanamycin (Km) resistant variant (10) of *Aminobacter*
108 sp. MSH1 (2) was used in this study. Unless specified otherwise, MSH1-GFP was grown on
109 R2A (13) or its broth version R2B (R2A with agar omitted from medium) supplemented with
110 200 mg/L BAM. MSH1-GFP was cryopreserved at -80°C prior to its use.

111 **Stability of BAM-mineralization in MSH1-GFP during short term growth on different media.**

112 For performing Experiment A (Step 1) (Table 1), MSH1-GFP was plated from the cryostock on
113 a R2A plate with 200 mg/L BAM and incubated for 4 days (25°C). A smear of colonies was
114 taken from the plate and suspended in 1 mL of 10 mM MgSO₄ isotonic solution. From the cell
115 suspension, 8 µL was inoculated in reaction tubes in triplicate containing 8 mL of either R2B,
116 R2B with 200 mg/L BAM or mineral salts (MS) medium (14) with 200 mg/L BAM. The cultures
117 were incubated at 25°C on a horizontal shaker until growth reached exponential phase at an
118 optical density at 660 nm (OD_{660nm}) of 0.1. The cultures were centrifuged (6000 x g, 15'),
119 washed three times with 10 mM MgSO₄ solution and resuspended in 10 mM MgSO₄. Cell
120 suspensions were serially diluted in 10 mM MgSO₄ and the dilutions plated on R2A plates
121 with 200 mg/L BAM. The plates were incubated at 25°C for 4 days. Ninety six colonies were
122 picked and transferred to separate wells in a sterile U96 Deepwell™ plate 2.0 mL (Nunc)
123 containing 100 µL MS medium amended with 3000 cpm of [Ring-U-¹⁴C]-labeled BAM (> 97%

124 purity) (Izotop, Institute of Isotopes Co., Ltd., Budapest, Hungary). The 96 well plates were
125 incubated at 25°C and the $^{14}\text{CO}_2$ produced in the wells from ^{14}C -BAM-mineralization was
126 measured after two weeks as described (15). For Experiment A (Step 2) (Table 1), part of the
127 culture grown in MS with 200 mg/L BAM in step 1 was transferred in triplicate (at a cell
128 density of 10^4 cells/mL) to reaction tubes containing 8 mL of either R2B, R2B with 200 mg/L
129 BAM and MS with 200 mg/L BAM. After incubation at 25°C for respectively 2, 2 and 7 days,
130 the cultures were harvested in the exponential phase at an $\text{OD}_{660\text{nm}}$ of 0.1, serially diluted in
131 10 mM MgSO_4 , and plated on R2A plates with 200 mg/L BAM. The plates were incubated for
132 5 days at 25°C and 96 colonies were examined for BAM-mineralization as explained above.
133 Amongst several BAM-mineralizing and none-BAM-mineralizing colonies, 10 were selected
134 and resuspended in 10 mM MgSO_4 . The cells were lysed by heating at 90°C for 30 min and
135 colony PCR was performed targeting the catabolic genes *bbdA*, *bbdD* and *bbdF* as described
136 below. Amplicons were separated by agarose gel electrophoresis (90 V, 45 min, 1.5%
137 agarose in TAE buffer) and visualized with an Ingeny Geldoc.

138 **Stability of the BAM-catabolic genotypes in a MSH1-GFP population during sequential**
139 **batch growth for up to 100 generations under varying conditions.** For Experiment B (Table
140 1), strain MSH1-GFP was grown on R2A plates with 200 mg/L BAM. A smear of MSH1-GFP
141 colonies was transferred to MS medium amended with 200 mg/L BAM and cultures were
142 incubated at 25°C for 7 days. Cultures were harvested at $\text{OD}_{660\text{nm}}$ of 0.1 by centrifugation
143 (6000 rpm, 15') and washed three times in 10 mM MgSO_4 . The cell suspension was diluted
144 and about 10^3 - 10^4 cells of strain MSH1-GFP were inoculated in triplicate in 4 mL of either
145 R2B, R2B with 20 mg/L BAM, R2B with 200 mg/L BAM or MS with 200 mg/L BAM. Cultures
146 were grown until an $\text{OD}_{660\text{nm}}$ of 0.4 (20 generations) in R2B, R2B with 20 mg/L BAM and R2B
147 with 200 mg/L BAM and until an $\text{OD}_{660\text{nm}}$ of 0.1 (18 generations) in MS with 200 mg/L BAM at

148 25°C. From these cultures, 10^3 - 10^4 cells were transferred to the same growth medium for
149 growing the next 18-20 generations. The cultures were as such transferred five times making
150 up at least 95 generations in total. At each transfer, the exact OD_{660nm} was determined and
151 samples of 1 mL were taken for DNA extraction. DNA was extracted using a cetyl
152 trimethylammonium bromide (CTAB) DNA extraction method (16) and the extracts were
153 analysed by qPCR targeting the MSH1 16S rRNA gene and the catabolic genes *bbdA*, *bddD*
154 and *bddF* as described below.

155 **Flow chamber experiment for assessing stability of BAM-catabolism in MSH1-GFP biofilms.**

156 Two experiments (Experiments C and D) (Table 1) employed the flow chamber setup
157 described by Weiss-Nielsen *et al.* (17) to grow MSH1-GFP biofilms in C and N starved
158 continuous conditions as reported by Sekhar *et al.* (10). In the first flow chamber experiment
159 (Experiment C), MSH1-GFP cell suspensions with either a high incidence of the BbdA⁺Dcba⁺
160 phenotype (designated as DCBA⁺ inoculum) or a high incidence of the BbdA⁺Dcba⁻
161 phenotype (designated as DCBA⁻ inoculum), were inoculated in triplicate flow channels
162 which were continuously fed with MS medium containing different nominal concentrations
163 of BAM, i.e., 1 mg/L, 100 µg/L, 10 µg/L, 1 µg/L or no BAM. The DCBA⁺ inoculum and
164 DCBA⁻ inoculum were obtained by cultivating a smear of MSH1-GFP colonies taken from a
165 R2A plate with 200 mg/L BAM, in, respectively R2B with 200 mg/L BAM (2 days) and MS with
166 200 mg/L BAM (7 days), at 25°C. Flow channels were inoculated with 4×10^7 MSH1-GFP cells
167 as described before (10). In the second flow chamber experiment (Experiment D), triplicate
168 flow channels were, as in Experiment C was set-up identical to Experiment D, except that the
169 AOC (extraneous to BAM) in the feed MS medium, estimated at around 100 µg/L in flow cell
170 experiment C, was reduced by overnight acid washing of the influent bottles with 2 N HCl
171 and rinsing three times with ultrapure water (MilliQ) (18). Estimations of MSH1-GFP biofilm

172 biomass showed that this resulted into a 3-fold reduction in AOC concentration in the feed,
173 i.e., around 20-30 $\mu\text{g/L}$ AOC (data not shown). In both experiments C and D, non-inoculated
174 control channels in triplicate were included for each BAM feed concentration to estimate
175 abiotic BAM removal and growth of contaminant microbiota. MSH1-GFP biofilms were in all
176 cases grown for four weeks and influent and effluent samples were taken regularly for
177 determining actual influent and effluent BAM concentrations using UPLC-UV/VIS (BAM > 1
178 $\mu\text{g/L}$) or UPLC-MS/MS (BAM < 1 $\mu\text{g/L}$) as described (10). BAM-degradation efficiency of the
179 systems was calculated as the difference between the residual concentration in the effluent
180 of the abiotic control and this in the inoculated flow channel as a percentage of the residual
181 concentration in the effluent of the abiotic control. Confocal Laser Scanning Microscopy
182 (CLSM) was used for the acquisition of 3D-images of MSH1-GFP biofilms at three locations in
183 the middle of the length of the flow channel at the end of the experiments as reported (10).
184 Images were only taken in the middle since previous work showed that biofilm structure and
185 colony size did not differ between different locations along the length of the flow channel
186 (10). The CLSM images allowed to assess biofilm biomass generated by MSH1-GFP and hence
187 to assess cell growth. For each system, nine image stacks (3 images in 3 replicates) of the
188 MSH1-GFP biofilms were used to calculate the total biofilm biovolume (μm^3) using COMSTAT
189 (19). Total biovolume values were used to calculate the total MSH1-GFP cell numbers in the
190 biofilm as described (10). After CLSM, MSH1-GFP biofilm cells in the flow channels were
191 collected by rinsing the channels with 10 mM MgSO_4 for CTAB DNA extraction(16). DNA
192 extracts were analysed with qPCR targeting the MSH1-GFP 16S rRNA gene *bbdA* and *bbdD* as
193 described below.

194 **BAM-catabolic stability in MSH1 in a bioaugmented pilot scale sand filter.** A pilot scale sand
195 filter experiment (Experiment E) (Table 1) was previously performed (20) to assess the

196 feasibility of bioaugmenting DWTP sand filter units with the wild type MSH1 for removing
197 BAM in the intake water until below the threshold limit of 0.1 µg/L. Detailed explanation
198 about the system and the operational parameters are described in Horemans *et al.* (20).
199 Influent BAM concentrations throughout the experiment were 0.19±0.04 µg/L. The sand
200 filters were inoculated with an MSH1 cell suspension derived from a culture either (i) grown
201 in R2B with 200 mg/L BAM for two days prior to inoculation or (ii) grown in MS with 200
202 mg/L BAM for 7 days and subsequently in R2B for 2 days (to maximize cell biomass) creating,
203 as in Experiments C and D, respectively a DCBA⁻ inoculum and a DCBA⁺ inoculum. Duplicate
204 samples of the effluent water and of the top layer (upper 20 cm layer) of the sand filters
205 were taken regularly from which DNA was extracted (20). Duplicate DNA extracts from
206 effluent and top layer sand filter material were used for qPCR analysis of *bbdD*.

207 **PCR and real time qPCR for the detection and quantification of the MSH1-GFP 16S rRNA,**
208 ***bbdA*, *bbdD* and *bbdF* genes.** PCR and qPCR used in this study targeted the *Aminobacter* sp.
209 MSH1 16S rRNA gene and the catabolic genes *bbdA*, *bbdD* and *bbdF*. *bbdA* encodes for the
210 conversion of BAM into 2,6-DCBA (12). Both *bbdD* and *bbdF* are involved in the degradation
211 of 2,6-DCBA. Biochemical and sequence analysis indicates that *bbdD* performs hydroxylation
212 of the aromatic moiety of 2,6-DCBA for preparation of ring-cleavage. Based on sequence
213 analysis, *bbdF* likely performs ring-cleavage. Colony PCR was performed on colonies
214 suspended in 100 µL UV-sterilized ultrapure water and heat lysed for 30 min at 95°C. PCR
215 reaction mixtures (50 µL) consisted of 0.25 µL *Taq* DNA polymerase (DreamTaq DNA
216 polymerase, Thermo Scientific), 2.5 µL of 10 µM forward primer, 2.5 µL of 10 µM reverse
217 primer (Table 2), 1 µL of 10 mM of each dNTP (Invitrogen), 5 µL 10x DreamTaq Green Buffer
218 (Thermo Scientific), 5 µL 1% BSA (bovine serum albumin), 30 µL PCR-H₂O and 1 µL of the
219 lysed colony suspension. The amplification reaction was 5 min at 94°C followed by 35 cycles

220 of 1 min at 94°C, 1 min at 59°C and 1 min at 72°C and ending with a final 5 min at 72°C. qPCR
221 was performed for each DNA sample in duplicate in a Rotor Gene Real-Time Centrifugal DNA
222 Amplification Apparatus (Corbett Research) using the SYBR Green detection method. The 15
223 µL reaction mixture contained 7.5 µL Absolute qPCR SYBR Green mix 2x (Thermo Scientific),
224 0.3 µL forward primer (200 nM), 0.3 µL reverse primer (200 nM) (Table 2), 3.9 µL nuclease
225 free water and 3 µL of template DNA. The amplification reactions included 15 min at 95°C
226 followed by 40 cycles of 20 s at 95°C, 20 s at 60°C and 20 s at 72°C. Fluorescence acquisition
227 was performed at each cycle after the elongation step at 72°C. Used DNA standards were
228 MSH1 16S rRNA gene, *bbdA*, *bbdD* and *bbdF* amplicons derived by conventional PCR from
229 MSH1 genomic DNA as described above but using 1 µL (10 ng) of MSH1 genomic DNA as
230 template and were serially diluted (10-fold) after purification from 10⁸ copies/µL until 1
231 copy/µL. Amplicon purification was done by agarose gel electrophoreses and subsequent gel
232 extraction using the QIAquick Gel Extraction Kit (Qiagen) followed by purification with the
233 Qiaquick PCR Purification Kit (Qiagen). DNA purity and concentrations were determined
234 using Qubit (ThermoFisher).

235 **Statistical analysis.** Significant differences (95% confidence interval) of BAM-degradation
236 efficiency, total MSH1-GFP cell numbers, ratios of *bbdA* and *bbdD* over 16S rRNA gene copies
237 and (specific) BAM-degradation rates between flow channels inoculated with a DCBA⁺ and
238 DCBA⁻ inoculum and between different feed conditions were determined with the unpaired
239 Student's T-test (significance at p<5%).

240 Results

241 **Stability of the BAM-catabolic phenotype in a MSH1-GFP population when grown under**
242 **varying conditions for a short term.** The effect of culturing conditions on the stability of the

243 BAM-mineralization phenotype in MSH1-GFP was determined by growing MSH1-GFP in
244 suspended batch under non-selective (R2B), semi-selective (R2B with 200 mg/L BAM) and
245 selective (MS with 200 mg/L BAM) conditions (Experiment A (Step 1)). Cells from each
246 culture were plated on R2A plates with 200 mg/L BAM and for each culturing condition, 90
247 colonies were individually suspended in MS medium containing BAM that was ^{14}C -labeled in
248 the aromatic moiety as sole C and energy source. The extent of BAM-mineralization
249 (percentage of $^{14}\text{C}\text{-CO}_2$ of $^{14}\text{C}\text{-BAM}$ added) was determined for each colony after two weeks
250 of incubation. Culturing MSH1-GFP in MS medium with BAM as only C-source had a clear
251 positive effect on the percentage of MSH1-GFP colonies that performed BAM-mineralization
252 (Table 3). To examine if a culture grown on MS with 200 mg/L BAM segregated into non-
253 mineralizing and mineralizing cells and how this depended on the medium composition, cells
254 originating from the culture grown on MS with 200 mg/L were transferred to the same three
255 media used in step 1 of Experiment A and grown until an $\text{OD}_{660\text{nm}}$ of 0.4 representing around
256 8 generations (Experiment A (Step 2)). The percentage of BAM-mineralizing colonies was
257 again highest (80%) for MSH1-GFP grown in MS with BAM but unexpectedly this percentage
258 did not decrease after growth in non-selective conditions (R2B without BAM). In contrast,
259 after growth in semi-selective conditions (R2B with BAM), only 33% of all tested colonies
260 showed mineralization indicating a clear impact of BAM on the percentage of the BAM-
261 mineralizing phenotype in case other C-sources are plentiful.

262 To investigate whether loss of the BAM-mineralization phenotype is linked to the loss of
263 specific BAM-catabolic genotypes, colony PCR was performed targeting the pBAM1 encoded
264 *bbdA* gene responsible for the BbdA^+ phenotype and *bbdD* and *bbdF* as markers for the two
265 pBAM2 encoded gene clusters that determine the Dcba^+ phenotype (and hence crucial for
266 mineralization of the aromatic moiety of BAM). MSH1-GFP colonies showing mineralization

267 of BAM always tested positive for all three genes. MSH1-GFP colonies showing no BAM-
268 mineralization tested negative for *bbdD* and *bbdF* but were positive for *bbdA* (data not
269 shown). These results show that lack of the BAM-mineralization phenotype is primarily
270 linked with the lack of the genes responsible for 2,6-DCBA degradation and that it involves
271 the loss of both gene clusters present on pBAM2 and possibly loss of pBAM2 in its entirety.

272 **Stability of the BAM-catabolic genotypes in a MSH1-GFP population during sequential**
273 **batch growth for up to 100 generations under varying conditions.** The lower percentage of
274 BAM-mineralizing MSH1-GFP colonies observed in Experiment A when MSH1-GFP was grown
275 in R2B with BAM compared to R2B was peculiar since the addition of BAM to R2B was
276 intended to retain the BAM-catabolic genes during culturing. To further examine this, MSH1-
277 GFP was grown in either R2B, R2B with 20 mg/L BAM and R2B with 200 mg/L BAM and also
278 in MS with 200 mg/L BAM for up to 100 generations, starting from a preculture grown on MS
279 with 200 mg/L BAM (Experiment B). For each growth condition, the loss of the catabolic
280 genotypes in function of the generation was quantified by means of qPCR targeting the
281 *Aminobacter* 16S rRNA gene, *bbdA* (as a marker of BbdA⁺) and *bbdD* (as a marker of Dcba⁺)
282 and determining the ratio of *bbdA* and *bbdD* abundance relative to the 16S rRNA gene copy
283 number (Figure 1). Only *bbdD* was used as a marker for the Dcba⁺ phenotype since *bbdD* and
284 *bbdF* were always lost together in Experiment A. The *bbdA*:16S rRNA gene and *bbdD*:16S
285 rRNA gene ratios in the culture used for inoculation were 2.3±0.8:1 and 3.0±1.3:1,
286 respectively. During growth in MS with BAM, the *bbdA*:16S rRNA and *bbdD*:16S rRNA gene
287 ratio changed to 2.4±0.6:1 and 0.5±0.1:1, respectively, at generation 95. In R2B, R2B with 20
288 mg/L BAM and R2B with 200 mg/L BAM, the ratio of *bbdA* over 16S rRNA gene copies did not
289 significantly change for 66 generations but significantly decreased between generation 66
290 and 100 by a factor 8, 7 and 6, respectively. In contrast, the ratio of *bbdD* over 16S rRNA

291 gene copies decreased already significantly between generation 0 and 18 and further
292 decreased during the following generations. Moreover, the loss of *bbdD* was clearly affected
293 by the BAM concentration as after 100 generations, the ratio *bbdD*:16S rRNA gene copies
294 had decreased by a factor 206, 1270 and 3003 in R2B, R2B with 20 mg/L BAM and R2B with
295 200 mg/L BAM, respectively.

296 **Stability of the BAM-catabolic genotype in MSH1-GFP in biofilms grown under continuous**
297 **C and N starved conditions in flow channels.** The results from the batch tests in high
298 nutrient conditions show that the BAM-catabolic phenotype in MSH1-GFP is prone to
299 genetic instability and that under non-selective conditions, MSH1-GFP cells that lack the
300 *Dcba*⁺ phenotype and only contain the *BbdA*⁺ phenotype rapidly outnumber BAM-
301 mineralizing cells. Furthermore, the presence of BAM increases the rate of loss of the *Dcba*⁺
302 phenotype. We questioned (i) whether MSH1 was also prone to loss of the *Dcba*⁺ phenotype
303 under the oligotrophic conditions of DWTPs that are substantially different from the high
304 nutrient conditions in the batch systems used in Experiments A and B but nevertheless
305 involve concentrations of BAM (around 1 µg/L) that are substantially lower than other AOC
306 (100 µg/L) and (ii) whether this was affected by the BAM concentration. Therefore, the
307 stability of the catabolic genotypes of MSH1-GFP when grown as a biofilm under C and N
308 starved conditions was investigated by determining the loss of *bbdA* and *bbdD* in MSH1-GFP
309 after growth in flow channels continuously fed with MS medium amended with different
310 concentrations of BAM representing micro- (1, 10, 100 µg/L) and macro-concentrations of
311 BAM (1000 µg/L BAM). As in Experiment B, loss of *bbdA* and *bbdD* was determined by
312 calculating the *bbdA*:16S rRNA and *bbdD*:16S rRNA gene ratio before and after growth in the
313 flow chambers (Experiment C). Furthermore, loss of the *BbdA*⁺ phenotype would directly
314 affect BAM degradation in the system, while loss of the *Dcba*⁺ phenotype will result into a

315 population of cells that lacks the ability to acquire energy and carbon from BAM and hence
316 might indirectly affect BAM degradation. Therefore, we examined degradation of BAM by
317 monitoring BAM concentration differences between influent and effluent and used CLSM to
318 determine MSH1 biomass in the flow cells. Together, this allowed to determine activity per
319 cell. Controls were included that were fed with MS medium without BAM. Furthermore, we
320 decided to inoculate the flow channels with MSH1-GFP cultures that were precultured either
321 on R2B with 200 mg/L BAM yielding an inoculum with a high incidence of BbdA⁺ Dcba⁻ cells
322 (DCBA⁻ inoculum) (*bbdA*:16S rRNA and *bbdD*:16S rRNA gene ratio of 2.6±0.4:1 and 0.1±0.0:1)
323 or on MS with 200 mg/L BAM yielding an inoculum with a high incidence of BbdA⁺ Dcba⁺ cells
324 (DCBA⁺ inoculum) (*bbdA*:16S rRNA and *bbdD*:16S rRNA gene ratio of 2.4±0.2:1 and
325 2.2±0.3:1). The two inocula were used to determine under which feed conditions the BbdA⁺
326 Dcba⁺ phenotype was lost (in case of the DCBA⁺ inoculum) or was enriched (in case of the
327 DCBA⁻ inoculum) in continuous systems.

328 Time lapse residual BAM concentrations in the effluent of flow channels inoculated with
329 either the DCBA⁻ inoculum or DCBA⁺ inoculum did not differ but depended on the feed BAM
330 concentration (Supplementary Material Figure S1). The BAM-degradation efficiency at the
331 end of the experiment was in the range of 70-85% (Table 4). MSH1-GFP biofilms consisted of
332 microcolonies of which the size (Figure 2) and total biomass (Table 4) were highly similar for
333 biofilms fed with MS without BAM and fed with MS containing BAM concentrations of 1, 10
334 and 100 µg/L indicating that residual AOC present in the medium was the main C source at
335 those BAM concentrations. Clearly larger colonies and higher biomass was recorded at feed
336 concentrations of 1000 µg/L BAM. Biomass values did not differ between systems inoculated
337 with the DCBA⁻ inoculum and those inoculated with the DCBA⁺ inoculum. The exception
338 were systems fed with 1000 µg/L BAM, where biofilms originating from the DCBA⁺ inoculum,

339 showed a slight but significantly higher biomass (factor 1.5) compared to biofilms developed
340 from the DCBA⁻ inoculum. Specific BAM-degradation rates were determined for each
341 condition at the end of the experiment and mainly depended on the feed BAM
342 concentration (Table 4). Only in case of a feed of 1000 µg/L BAM, a slight but significant
343 difference (factor 1.5 higher) in specific degradation rate was found for systems inoculated
344 with the DCBA⁻ inoculum compared to systems inoculated with the DCBA⁺ inoculum.

345 The *bbdA*:16S rRNA gene ratio at the end of the experiment did not significantly differ from
346 that of the inoculum for any of the implemented growth conditions and as such did not
347 differ (i) between biofilms grown on different BAM concentrations, and (ii) between biofilms
348 originating from a DCBA⁻ inoculum or DCBA⁺ inoculum (Table 4 and Figure 3). The *bbdD*:16S
349 rRNA gene ratio, however, clearly changed. In biofilms originating from the DCBA⁺ inoculum,
350 the *bbdD*:16S rRNA gene ratio had decreased significantly (factor 7, 10, 8, 12 and 2 in case of
351 feeds containing 0, 1, 10, 100 and 1000 µg/L BAM, respectively). Similarly, biofilms
352 originating from the DCBA⁻ inoculum became depleted in *bbdD* when grown on 0, 1 and 10
353 µg/L BAM (factor 4, 3 and 4, respectively). In contrast, the DCBA⁻ inoculum biofilms became
354 enriched in *bbdD* when grown on 100 and 1000 µg/L BAM (factor 2 and 5, respectively). The
355 results show that, as in high nutrient batch systems, the presence of additional C-sources
356 results into the loss of especially *bbdD* in MSH1-GFP under the N and C limiting conditions of
357 a DWTP. Loss of *bbdA* was, however, not observed and BAM removal rates were not
358 affected.

359 **Stability of the BAM-catabolic genotype in MSH1-GFP in biofilms grown under C and N**
360 **starved conditions in flow channels: elucidating the effect of AOC.** To obtain more
361 information on the role of residual AOC in the loss of *bbdD* in the flow chambers in

Experiment C, a second flow chamber experiment (Experiment D, Table 1) was initiated with a setup that was identical to this in Experiment C but in which the AOC content in the feed was reduced by a factor 3 (final AOC content was estimated at 20-30 $\mu\text{g/L}$ AOC). As in Experiment C, the systems were inoculated with either a DCBA⁻ inoculum (*bbdA*:16S rRNA and *bbdD*:16S rRNA gene ratio of respectively $2.67\pm 0.33:1$ and $0.03\pm 1:1$) and a DCBA⁺ inoculum (*bbdA*:16S rRNA and *bbdD*:16S rRNA gene ratio of respectively $2.70\pm 0.43:1$ and $2.77\pm 0.21:1$) (Table 4 and Figure 3). Reducing the AOC content was expected to result into reduced non-selective growth and minimal loss of the Dcba⁺ phenotype. This was indeed the case. As in Experiment C, MSH1-GFP biofilms were characterized by microcolonies that only became more substantial in size compared to the feed condition without BAM, when BAM was added in the feed at 1000 $\mu\text{g/L}$. Biofilm biomass estimations (Table 4) showed that significantly less biofilm biomass (factor 2.5) was produced when AOC was reduced in the feed compared to when AOC was not reduced (Experiment C). The reduced growth had a clear effect on BAM degradation where in contrast to Experiment C, a linear and slower decrease in the residual BAM concentration was observed (Supplementary Material Figure S1). As in Experiment C, the *bbdA*:16S rRNA ratios did not change compared to the inoculum in any of the conditions (Table 4 and Figure 3). However, in contrast to Experiment C, the *bbdD*:16S rRNA ratios in the biofilms originating from the DCBA⁺ inoculum was not significantly different from that of the inoculum for any of the BAM feed conditions, neither it was in biofilms originating from the DCBA⁻ inoculum in systems fed with 0, 1 and 10 $\mu\text{g/L}$ BAM. In systems inoculated with the DCBA⁻ inoculum receiving 100 and 1000 $\mu\text{g/L}$ BAM, the *bbdD*:16S rRNA gene ratio had again increased (factor 6 and 60, respectively).

Stability of the BAM-catabolic genotypes in MSH1 in bioaugmented pilot DWTP sand filters. In a previous study, both a MSH1-GFP culture with a high incidence of the BAM⁺

386 DCBA⁺ phenotype (DCBA⁺ inoculum), and a MSH1-GFP culture with a high incidence in BAM⁺
387 DCBA⁻ phenotype (DCBA⁻ inoculum), were used for bioaugmentation of pilot DWTP sand
388 filters to treat groundwater contaminated with BAM at a concentration of 0.2 µg/L (20)
389 (Experiment E). The *bbdA*:16S rRNA and *bbdD*:16S rRNA gene ratio was estimated at
390 0.50±0.05:1 and 0.10±0.02:1 in the DCBA⁻ inoculum and 0.55±0.10:1 and 0.71±0.05:1 for the
391 DCBA⁺ inoculum. The *bbdA*:16S rRNA gene ratios were previously determined in effluent and
392 top layer sand filter samples during reactor operation and did not change in neither the
393 reactor inoculated with the DCBA⁻ or DCBA⁺ inoculum (20) (Figure 4). Similarly, the *bbdD*:16S
394 rRNA gene ratio did not change in the top layer samples and effluent samples (both on
395 average 0.01±0.01:1) of the reactor inoculated with the DCBA⁻ inoculum. The *bbdD*:16S rRNA
396 gene ratio in the top layer and effluent samples of the system inoculated with the DCBA⁺
397 inoculum, decreased significantly in time to 0.01±0.00:1 in the top layer samples and to
398 0.04±0.00:1 in effluent samples by the end of operation.

399 Discussion

400 In this study, we show evidence that strain *Aminobacter* sp. MSH1 which is a candidate
401 catalyst for application in DWTPs for removal of the common groundwater pollutant BAM,
402 rapidly shows a high incidence of cells that lack the BAM-mineralization phenotype when
403 carbon sources other than BAM are present in the growth medium. Lack of the BAM-
404 mineralization capacity in MSH1-GFP cells is in the first place due to the lack of the DCBA⁺
405 phenotype due to a loss of catabolic genes associated with pBAM2. The BbdA⁺ phenotype
406 appears more stable. As a result, when conditions are non-selective, cells will develop that
407 lack the catabolic genotype for full BAM-mineralization but still degrade BAM to 2,6-DCBA.
408 Instability of organic xenobiotic catabolic genes in organic xenobiotic degrading bacteria has

409 been reported frequently and is either due to intramolecular gene rearrangements or
410 complete plasmid loss (21-23). Our experiments show that loss of *bbdD* is concomitant with
411 loss of *bbdF* indicating that both gene clusters on pBAM2 are simultaneously lost. Whether
412 this is due to loss of the entire plasmid is currently unclear but PCR analysis of Dcba⁻ mutants
413 of MSH1 targeting the pBAM2 backbone genes indicate that this is the case (T'Syen,
414 unpublished). Regarding loss of the BbdA⁺ phenotype, we have previously shown that in a
415 BbdA⁻ mutant, the strain contains a deleted version of pBAM1 which misses the whole
416 accessory gene region indicating that the whole plasmid pBAM1 is not necessarily lost (12).
417 Further increase of incidence of the Dcba⁻ variant during growth of MSH1-GFP can be either
418 due to the above mentioned genetic instability during cell division or due to growth rate
419 advantage of the Dcba⁻ cells over Dcba⁺ cells. The latter was observed in *Pseudomonas*
420 *putida* hosting plasmid pTDN1 encoding the degradation of aromatic amines (TDN⁺
421 phenotype). Initial loss of the TDN⁺ phenotype was due to either a recombinational deletion
422 or complete plasmid loss. (24). Similar observations were reported for pWW100 inferring
423 biphenyl metabolism (BPH⁺) (25) and pWWO-1 inferring toluene degradation (TOL⁺) (26) in
424 *P. putida*. Metabolic burden related to extra DNA/plasmid replication (27, 28) is suggested as
425 a major reason for growth retardation of plasmid bearing cells compared to cured cells (24).
426 Since in this study we always started from colonies grown on non-selective plates, the
427 precise mechanism of propagation of the Dcba⁻ phenotype is not clear. Based on the
428 generation experiment (experiment B), we calculated that to obtain the 42% difference in
429 the *bbdD*:16S rRNA gene ratio between generation 19 and 66, the Dcba⁻ phenotype should
430 have a growth rate that is a factor 1.1 higher than the Dcba⁺ phenotype and hence growth
431 advantage is a plausible explanation. On the other hand, based on growth rate of both
432 phenotypes and the proportion of each phenotype at 66 generations, the *bbdD*:16S rRNA

433 gene ratio in the inoculum should have been 0.72:1. However, this was not the case as 3:1
434 was measured which indicates that only a very low fraction of the start population did not
435 contain *bddD*. Hence genetic instability likely contributed to the propagation of the Dcba⁻
436 phenotype at least at the start of the generation experiment. Interestingly, the rate of
437 incidence of the Dcba⁻ phenotype during growth in R2B, increased when BAM was amended.
438 Likely, the metabolic burden in MSH1-GFP cells is higher in the presence of BAM. Proteomic
439 analysis suggests the increased production of the enzymes encoded by the *bddFGHIJK* gene
440 cluster in MSH1 in the presence of BAM and 2,6-DCBA (T'Syen, unpublished) as well as of
441 several stress proteins (T'Syen, unpublished). The presence of BAM or the expression of the
442 metabolic machinery might bring MSH1-GFP into a stress situation what might affect growth
443 rates of the cell or genetic instability. Some authors reported the possibility that production
444 of GFP can exert a metabolic burden on cells that carry *gfp* which might hence increase
445 catabolic gene loss in the MSH1-GFP population. However, this is unlikely since Sekhar *et al.*
446 (10) showed growth rates and biofilm formation of the MSH1-GFP that did not differ from
447 those of the wild type strain. As such, no metabolic burden was expected from GFP-
448 production which is in agreement with observations in other organisms (29, 30). Therefore,
449 we assume that conclusions regarding instability of the BAM catabolic phenotype/genotype
450 in MSH1-GFP can be extrapolated to the wild type MSH1.

451 Upon growth on BAM, the proportion of cells carrying both gene clusters increased and
452 *bddD* and *bddA* levels were even attained that were respectively 2 to 3-fold higher than that
453 of the 16S rRNA gene copy number. This is probably due to the presence of multiple plasmid
454 copies per cell. Reported plasmid copy numbers per cell of IncP1 plasmids and of *repABC*
455 plasmids are around 2-6 and 1-5 (31), respectively, *Aminobacter* genomes (accession

456 PRJNA316647) have three 16S rRNA gene copies, suggesting that the fraction of MSH1 cells
457 having a Dcba⁺ and hence BAM-mineralization genotype/phenotype is two-fold lower than
458 indicated by the *bbdD*:16S rRNA gene ratio.

459 The observation of loss of the BAM-catabolic phenotype and in particularly the Dcba⁺
460 phenotype under non-selective conditions might have implications for the use of MSH1 in
461 bioaugmentation of DWTP filter units. This relates first of all to its cultivation in high nutrient
462 conditions to produce sufficient biomass for bioaugmentation. Recently, Schultz-Jensen *et*
463 *al.* (32) presented optimal conditons for culturing MSH1 at high densities. The authors
464 cultured the strain using glucose as the non-selective C-source and according to our
465 calculations, the Dcba⁺ phenotype could have dropped to 5 % of the total MSH1 population.
466 The propagated final MSH1 suspension in its entirety tested positive for BAM-mineralization,
467 but the BAM-catabolic capacity at the single-cell level was not tested (32). During cultivation
468 prior to bioaugmentation, MSH1 cultures need to be monitored for the occurrence of the
469 Dcba⁺ phenotype and preferably precultured in selective conditions prior to mass-cultivation
470 in reactors.

471 As important for bioaugmentation are the consequences of the catabolic instability for the
472 strain's actual performance in DWTP biofilter units where conditions are not necessarily
473 selective, i.e., BAM is present at trace concentrations and other non-selective AOC is
474 expected to be a factor 20 to 100 higher (9, 18, 33, 34). The retention of the BbdA⁺
475 phenotype but loss of the Dcba⁺ phenotype implicates that BAM is still degraded to 2,6-
476 DCBA by MSH1-GFP but impaired in further DCBA conversion. It also implicates that the
477 Dcba⁻ phenotype will not gain energy nor carbon from BAM in the highly oligotrophic
478 environment of DWTP biofilters. Major questions were whether (i) observations in nutrient

rich medium conditions can be translated to starvation conditions, i.e. whether loss also occurs under the oligotrophic conditions of a DWTP and (ii) whether an inoculum with a high incidence of BbdA⁺ Dcba⁻ cells affects BAM-degradation and performs differently compared to an inoculum with a high incidence of BbdA⁺ Dcba⁺ cells regarding BAM-degradation under the oligotrophic conditions of a DWTP. In our study, these questions were examined under controlled conditions in flow channels by exploring the activity and abundances of BbdA⁺ Dcba⁻ and BbdA⁺ Dcba⁺ MSH-GFP populations under carbon and N limited feed conditions. Based on previous records of initial cell attachment of MSH1 and AOC estimations (10), we calculated that at the end of experiment C, the AOC in the feed supported 70 generations of MSH1-GFP. At the end of the experiment, the BbdA⁺ Dcba⁺ phenotype occurred at a ratio of 0.2:1 *bbdD*:16S rRNA gene copies for MSH1-GFP grown in flow channels fed with 0, 1, and 10 µg/L BAM and 0.1:1 when grown in flow channels fed with 100 µg/L BAM when starting from a DCBA⁺ inoculum. These numbers correspond remarkably well with the *bbdD*:16S rRNA gene ratio after 70 generations in experiment B in nutrient rich conditions, suggesting that the Dcba⁺ genotype is as efficiently lost under continuous C and N starved conditions when AOC is present in surplus to BAM. This is supported by Experiment D, where growth of MSH1-GFP was restrained by reducing AOC and were no reduction in the *bbdD*:16S rRNA gene ratio was observed in MSH1-GFP biofilms compared to the inoculum. Apparently, a metabolic burden also weighs on growth of the BbdA⁺ Dcba⁺ phenotype in MSH1-GFP biofilms in starved conditions. However, the presence of BAM did not affect the incidence of the BbdA⁺ Dcba⁺ phenotype which is in contrast to what was observed in nutrient rich conditions tested in batch. In R2B with 20 mg/L BAM and 200 mg/L BAM, the percentage of AOC derived from BAM to AOC derived from R2B is estimated at 1% and 10% and is hence comparable with this in the biofilms fed with 10 and 100 µg/L BAM. Possibly, the BbdA⁺

503 Dcba⁺ phenotype does not undergo an extra metabolic burden when BAM is present at
504 micropollutant concentrations. At feed concentrations of 1000 µg/L BAM, the relative
505 abundance of the BbdA⁺ Dcba⁺ phenotype in flow chambers inoculated with the DCBA⁺
506 population remained high. At these concentrations BAM is in surplus to other C and
507 apparently functions as a main and selective C source. This is supported by the results with
508 the DCBA⁻ inoculum that clearly increased in BbdA⁺ Dcba⁺ incidence when grown on 1000
509 µg/L and 100 µg/L BAM. We can conclude that a surplus of AOC compared to BAM in intake
510 groundwater contaminated with trace BAM concentrations might lead to loss of the BbdA⁺
511 Dcba⁺ phenotype in DWTP filtration units. This was confirmed by the pilot scale sand filter
512 experiment, where intake groundwater contained BAM at 0.2 µg/L and AOC at 25 µg/L and
513 also clear loss of the Dcba⁺ phenotype was observed when starting with an inoculum with a
514 high incidence of BbdA⁺ Dcba⁺ cells. The long term fate of the Dcba⁺ phenotype and whether
515 it will completely disappear from the system is currently unclear.

516 Based on biovolume calculations of MSH1-GFP biofilms, specific BAM-degradation rates at
517 micropollutant concentrations were the same in both flow chamber experiments (with and
518 without reduction of AOC) as those reported by Sekhar *et al.* (10) and hence were 100-fold
519 lower than those found for fresh cells in suspended batch conditions. Instability of the Dcba⁺
520 phenotype could be a cause of reduced activity since it will result into cells that cannot gain
521 energy from the available BAM. However, while the abundance of the BbdA⁺ Dcba⁺
522 phenotype was significantly higher in biofilms originating from the DCBA⁺ inoculum
523 compared to biofilms originating from the DCBA⁻ inoculum, no significant difference in the
524 specific BAM-degradation activity was observed when fed with either 1, 10 or 100 µg/L BAM.
525 As such, the specific BAM-degradation activity at micropollutant concentrations of BAM
526 (<100 µg/L BAM) was not influenced by the abundance of the BbdA⁺ Dcba⁺ phenotype in the

527 biofilms. As such, we hypothesize that the energy derived from BAM at those trace level
528 concentrations does not substantially add to the energy gained from AOC which is sufficient
529 to sustain BAM-degrading activity by BbdA. The low incidence of the Dcba⁺ phenotype in the
530 MSH1-GFP cell population nevertheless raises concern about the mineralization of BAM and
531 possible production of DCBA in the system which was not determined in this study and other
532 studies (10, 20). An imbalance in BAM-mineralizing cells and DCBA-producing cells can lead
533 to the partial accumulation of DCBA during bioremediation. The presence of indigenous
534 microbiota mineralizing 2,6-DCBA bacteria in the sand filter as shown for some sand filters of
535 DWTPs receiving BAM might solve this problem (35).

536 Acknowledgements

537 This work was supported by EU FP7 project Biotreat n°: 266039, FWO post-doctoral fellow
538 grant 12Q0215N to B.H., BELSPO IAP-project μ -manager n° P7/25 and KULeuven C1 project
539 n° C14/15/043. We thank K. Simoens for excellent help in DNA extraction and real time
540 qPCR.

541 References

- 542 1. Clausen L, Arildskov NP, Larsen F, Aamand J, Albrechtsen H-J. 2007. Degradation of the
543 herbicide dichlobenil and its metabolite BAM in soils and subsurface sediments. *J Contam*
544 *Hydrol* **89**:157-173.
- 545 2. Sørensen SR, Holtze MS, Simonsen A, Aamand J. 2007. Degradation and mineralization of
546 nanomolar concentrations of the herbicide dichlobenil and Its persistent metabolite 2,6-
547 dichlorobenzamide by *Aminobacter* spp. isolated from dichlobenil-treated soils. *Appl Environ*
548 *Microbiol* **73**:399-406.
- 549 3. EU. 1998. Council Directive 98/83/EC of 3 November 1998 on the quality of water intended
550 for human consumption. Council of the European Union.
- 551 4. Schwarzenbach R, Escher BI, Fenner K, Hofstetter TB, Johnson CA, von Gunten U, Wehrli B.
552 2006. The challenge of micropollutants in aquatic systems. *Science* **313**:1072-1077.
- 553 5. Hernández-Leal L, Temmink H, Zeeman G, Buisman CJ. 2011. Removal of micropollutants
554 from aerobically treated grey water via ozone and activated carbon. *Water Resources*
555 **45**:2887-2896.

- 556 6. **Reungoat J, Macova M, Escher BI, Carswell S, Mueller JF, Keller J.** 2009. Removal of
557 micropollutants and reduction of biological activity in a full scale reclamation plant using
558 ozonation and activated carbon filtration. *Water Res* **44**:625-637.
- 559 7. **Benner J, Helbling DE, Kohler H-PE, Wittebol J, Kaiser E, Prasse C, Ternes TA, Albers CN,**
560 **Aamand J, Horemans B, Springael D, Walravens E, Boon N.** 2013. Is biological treatment a
561 viable alternative for micropollutant removal in drinking water treatment processes? *Water*
562 *Res* **47**:5955-5976.
- 563 8. **Vandermaesen J, Horemans B, Bers K, Vandermeeren P, Herrmann S, Sekhar A, Seuntjens**
564 **P, Springael D.** 2016. Application of biodegradation in mitigating and remediating pesticide
565 contamination of freshwater resources: state of the art and challenges for optimization. *Appl*
566 *Microbiol Biotechnol* **100**:7361-7376.
- 567 9. **Albers CN, Feld L, Ellegaard-Jensen L, Aamand J.** 2015. Degradation of trace concentrations
568 of the persistent groundwater pollutant 2,6-dichlorobenzamide (BAM) in bioaugmented
569 rapid sand filters. *Water Res* **83**:61-70.
- 570 10. **Sekhar A, Horemans B, Aamand J, Sørensen SR, Vanhaecke L, Bussche JV, Hofkens J,**
571 **Springael D.** 2016. Surface colonization and activity of the 2,6-dichlorobenzamide (BAM)
572 degrading *Aminobacter* sp. strain MSH1 at macro- and micropollutant BAM concentrations.
573 *Environ Sci Technol* **50**:10123-10133.
- 574 11. **Top EM, Springael D, Boon N.** 2002. Catabolic mobile genetic elements and their potential
575 use in bioaugmentation of polluted soils and waters. *FEMS Microbiol Ecol* **42**:199-208.
- 576 12. **T'Syen J, Tassoni R, Hansen L, Sorensen SJ, Leroy B, Sekhar A, Wattiez R, De Mot R,**
577 **Springael D.** 2015. Identification of the amidase BbdA that initiates biodegradation of the
578 groundwater micropollutant 2,6-dichlorobenzamide (BAM) in *Aminobacter* sp. MSH1.
579 *Environ Sci Technol* **49**:11703-11713.
- 580 13. **Reasoner DJ, Geldreich EE.** 1985. A new medium for the enumeration and subculture of
581 bacteria from potable water. *Appl Environ Microbiol* **49**:1-7.
- 582 14. **Sørensen SR, Aamand J.** 2003. Rapid mineralisation of the herbicide isoproturon in soil from
583 a previously treated Danish agricultural field. *Pest Manage Sci* **59**:1118-1124.
- 584 15. **Johnsen AR, Hybholt TK, Jacobsen OS, Aamand J.** 2009. A radiorespirometric method for
585 measuring mineralization of [¹⁴C]-compounds in a 96-well microplate format. *J Microbiol*
586 *Methods* **79**:114-116.
- 587 16. **Larsen MH, Biermann K, Tandberg S, Hsu T, Jacobs WR.** 2005. Genetic manipulation of
588 *Mycobacterium tuberculosis*, *Current Protocols in Microbiology*. John Wiley & Sons, Inc.
- 589 17. **Weiss Nielsen M, Sternberg C, Molin S, Regenberg B.** 2011. *Pseudomonas aeruginosa* and
590 *Saccharomyces cerevisiae* biofilm in flow cells. . *J Vis Exp*:e2383.
- 591 18. **Charnock C, Kjønne O.** 2000. Assimilable organic carbon and biodegradable dissolved organic
592 carbon in Norwegian raw and drinking waters. *Water Res* **34**:2629-2642.
- 593 19. **Heydorn A, Nielsen AT, Hentzer M, Sternberg C, Givskov M, Ersbäll BK, Molin S.** 2000.
594 Quantification of biofilm structures by the novel computer program COMSTAT. *Microbiology*
595 **146**:2395-2407.
- 596 20. **Horemans B, Raes B, Vandermaesen J, Simanjuntak Y, Brocatus H, T'Syen J, Degryse J,**
597 **Boonen J, Wittebol J, Lapanje A, Sorensen SR, Springael D.** 2016. Biocarriers improve
598 bioaugmentation efficiency of a rapid sand filter for the treatment of 2,6-dichlorobenzamide
599 (BAM)-contaminated drinking water. *Environ Sci Technol* doi: 10.1021/acs.est.1026b05027.
- 600 21. **Wyndham RC, Singh RK, Straus NA.** 1988. Catabolic instability, plasmid gene deletion and
601 recombination in *Alcaligenes* sp. BR60. *Arch Microbiol* **150**:237-243.
- 602 22. **Cérémonie H, Boubakri H, Mavingui P, Simonet P, Vogel TM.** 2006. Plasmid-encoded γ -
603 hexachlorocyclohexane degradation genes and insertion sequences in *Sphingobium*
604 *francense* (ex-*Sphingomonas paucimobilis* Sp+). *FEMS Microbiol Lett* **257**:243-252.
- 605 23. **Brown VR, Knapp JS, Heritage J.** 1990. Instability of the morpholine-degradative phenotype
606 in mycobacteria isolated from activated sludge. *J Appl Bacteriol* **69**:54-62.

- 607 24. **Saint CP, Venables WA.** 1990. Loss of Tdn catabolic genes by deletion from and curing of
608 plasmid pTDN1 in *Pseudomonas putida*: rate and mode of loss are substrate and pH
609 dependent. *Microbiology* **136**:627-636.
- 610 25. **Lloyd-Jones G, de Jong C, Ogden RC, Duetz WA, Williams PA.** 1994. Recombination of the
611 *bph* (biphenyl) catabolic genes from plasmid pWW100 and their deletion during growth on
612 benzoate. *Appl Environ Microbiol* **60**:691-696.
- 613 26. **Duetz WA, van Andel JG.** 1991. Stability of TOL plasmid pWW0 in *Pseudomonas putida* mt-2
614 under non-selective conditions in continuous culture. *J Gen Microbiol* **137**:1369-1374.
- 615 27. **Nojiri H.** 2013. Impact of catabolic plasmids on host cell physiology. *Curr Opin Biotechnol*
616 **24**:423-430.
- 617 28. **Rozkov A, Avignone-Rossa CA, Ertl PF, Jones P, O'Kennedy RD, Smith JJ, Dale JW, Bushell
618 ME.** 2004. Characterization of the metabolic burden on *Escherichia coli* DH1 cells imposed by
619 the presence of a plasmid containing a gene therapy sequence. *Biotechnol Bioeng* **88**:909-
620 915.
- 621 29. **Bloemberg GV, O'Toole GA, Lugtenberg BJ, Kolter R.** 1997. Green fluorescent protein as a
622 marker for *Pseudomonas* spp. *Appl Environ Microbiol* **63**:4543-4551.
- 623 30. **Dandie CE, Thomas SM, McClure NC.** 2001. Comparison of a range of green fluorescent
624 protein-tagging vectors for monitoring a microbial inoculant in soil. *Lett Appl Microbiol*
625 **32**:26-30.
- 626 31. **Cevallos MA, Cervantes-Rivera R, Gutiérrez-Ríos RM.** 2008. The *repABC* plasmid family.
627 *Plasmid* **60**:19-37.
- 628 32. **Schultz-Jensen N, Knudsen BE, Frkova Z, Aamand J, Johansen T, Thykaer J, Sørensen SR.**
629 2014. Large-scale bioreactor production of the herbicide-degrading *Aminobacter* sp. strain
630 MSH1. *Appl Microbiol Biotechnol* **98**:2335-2344.
- 631 33. **Bradford SM, Palmer CJ, Olson BH.** 1994. Assimilable organic carbon concentrations in
632 Southern California surface and groundwater. *Water Res* **28**:427-435.
- 633 34. **Björklund E, Anskjær GG, Hansen M, Styriehave B, Halling-Sørensen B.** 2011. Analysis and
634 environmental concentrations of the herbicide dichlobenil and its main metabolite 2,6-
635 dichlorobenzamide (BAM): A review. *Sci Total Environ* **409**:2343-2356.
- 636 35. **Vandermaesen J, Horemans B, Degryse J, Boonen J, Walravens E, Springael D.** 2016.
637 Mineralization of the common groundwater pollutant 2,6-dichlorobenzamide (BAM) and its
638 metabolite 2,6-dichlorobenzoic acid (2,6-DCBA) in sand filter units of drinking water
639 treatment plants. *Environ Sci Technol* **50**:10114-10122.
- 640 36. **Marchesi JR, Sato T, Weightman AJ, Martin TA, Fry JC, Hiom SJ, Wade WG.** 1998. Design and
641 evaluation of useful bacterium-specific PCR primers that amplify genes coding for bacterial
642 16S rRNA. *Appl Environ Microbiol* **64**:795-799.

643

644

645 **Tables**

646 Table 1. Overview of the experiments to assess BAM-catabolic stability in MSH1-GFP and MSH1

	Origin of inoculum	Culturing conditions	Setup	Assessment
Experiment A	BAM-mineralization stability of MSH1-GFP during short term growth			
Step 1	Smear of MSH1-GFP colonies on R2A plate amended with 200 mg/L BAM	<ul style="list-style-type: none"> MS with 200 mg/L BAM R2B with 200 mg/L BAM R2B 	Suspended batch	<ul style="list-style-type: none"> Colony screening for ^{14}C-BAM-mineralization Colony PCR for <i>bddA</i>, <i>bddD</i> and <i>bddF</i>
Step 2	MSH1-GFP cells cultured in MS with 200 mg/L BAM (Step 1)	<ul style="list-style-type: none"> MS with 200 mg/L BAM R2B with 200 mg/L BAM R2B 	Suspended batch	
Experiment B	Stability of the BAM-catabolic genotype during sequential batch growth			
	MSH1-GFP cells cultured in MS with 200 mg/L BAM	<ul style="list-style-type: none"> MS with 200 mg/L BAM R2B with 200 mg/L BAM R2B with 20 mg/L BAM R2B 	Suspended batch	<ul style="list-style-type: none"> Real time qPCR quantification of <i>bddA</i>, <i>bddD</i> and MSH1 16S rRNA gene in function of generation
Experiment C	BAM-catabolic stability of MSH1-GFP in C and N starved conditions			
	MSH1-GFP cells cultured in MS with 200 mg/L BAM	MS medium	Continuously fed flow chamber	<ul style="list-style-type: none"> Real time qPCR for quantification of <i>bddA</i>, <i>bddD</i> and MSH1 16S rRNA gene BAM-degradation efficiency Biofilm biomass
	MSH1-GFP cells cultured in R2B with 200 mg/L BAM	<ul style="list-style-type: none"> with no BAM with 1 $\mu\text{g/L}$ BAM with 10 $\mu\text{g/L}$ BAM with 100 $\mu\text{g/L}$ BAM with 1000 $\mu\text{g/L}$ BAM 		

				quantification using CLSM
Experiment D	BAM-catabolic stability of MSH1-GFP in C and N starved conditions: AOC depletion in feed			
	MSH1-GFP cells cultured in MS with 200 mg/L BAM	AOC-depleted MS medium <ul style="list-style-type: none">with no BAMwith 1 µg/L BAMwith 10 µg/L BAMwith 100 µg/L BAMwith 1000 µg/L BAM	Continuously fed flow chamber	<ul style="list-style-type: none">Real time qPCR for quantification of <i>bbdA</i>, <i>bbdD</i> and MSH1 16S rRNA geneBAM-degradation efficiencyBiofilm biomass quantification using CLSM
	MSH1-GFP cells cultured in R2B with 200 mg/L BAM			
Experiment E	BAM-catabolic stability in a pilot scale reactor*			
	MSH1-GFP cells cultured in MS with 200 mg/L BAM	Groundwater containing 0.2 µg/L BAM	Pilot scale DWTP sand filter	Real time qPCR for quantification of <i>bbdA</i> , <i>bbdD</i> and MSH1 16S rRNA gene
	MSH1-GFP cells cultured in MS with 200 mg/L BAM and then in R2B with 200 mg/L BAM			

647

* : Horemans et al. (20)

647 * : Horemans et al. (20)

648 Table 2: PCR and qPCR primers used in this study for detecting and quantifying the MSH1-GFP 16S
 649 rRNA gene and the BAM-catabolic genes *bbdA*, *bbdD* and *bbdF*. Primers for qPCRs are indicated with
 650 RT (real-time).

Target	Primers (F and R)	Sequences	Fragment size (bp)
16S rRNA of MSH1	27F*	ACCGTATACGTCCGATAGGA	1465
	1492R*	CTCGGACTCTAGATTGCCAG	
	MSH1 F RT	CAACCTTCGCCCTTAGTTGC	83
	MSH1 R RT	TCATCTTCACCTTCCTCGCG	
<i>bbdA</i>	<i>bbdA</i> -F1	ATGCCCAGTGGTGCAAATCTGCCA	1557
	<i>bbdA</i> -R1543	CTTCTTGCGCCAATCCCAGACTT	
	AmiF RT	ATATCACGGCCGGTACTATGCCAA	156
<i>bbdD</i>	AmiR RT	TCTTCCAAGATCGAACAACCCGGA	614
	C11_ringdiox_509F	ATAGTGCGTTGTGTTGCGTGTTTC	
	C11_ringdiox_1099R	AGGTGATCGGTGAGGGTATTCACT	146
	C11 ringdiox F RT	CCGAGCTGTTGGTTTCATCG	
<i>bbdF</i>	C11 ringdiox R RT	GATCTTCAATACGCCGCTGG	435
	C6_23diox_1833F	GCTTTTCCCATTTGTTGAGCGTT	
	C6_23diox_2244R	CGGTCCTGTTGAGCATTGACTTT	

651 *: Universal bacterial primer pair targeting the 16S rRNA gene in bacteria (36). F: forward
 652 primer; R: reverse primer.

653 Table 3. Percentage of MSH1-GFP colonies that showed mineralization of BAM ($> 5\%$ $^{14}\text{C-CO}_2$
654 production) or no mineralization ($< 5\%$ $^{14}\text{C-CO}_2$ production) when transferred to MS with $^{14}\text{C-BAM}$.
655 Colonies originated from R2A plates containing 200 mg/L BAM after (i) plating of MSH1-GFP cells
656 cultured in triplicate in R2B, R2B with 200 mg/L BAM and MS with 200 mg/L BAM that were
657 inoculated with a smear of MSH1-GFP colonies growing on a R2A plate with 200 mg/L BAM
658 (Experiment A (Step 1) (Table 1)) or (ii) plating of MSH1-GFP cells cultured in triplicate in R2B, R2B
659 with 200 mg/L BAM and MS with 200 mg/L BAM that were inoculated with a MSH1-GFP culture
660 grown in MS with 200 mg/L BAM (Experiment A (Step 2) (Table 1)).

	Percentage of tested colonies	
	Mineralization	
	No	Yes
Inoculated with smear of MSH1-GFP		
R2B	90 \pm 7%	10 \pm 7%
R2B with BAM	95 \pm 4%	5 \pm 4%
MS with BAM	12 \pm 9%	88 \pm 9%
Inoculated from culture grown on MS		
R2B	11 \pm 10%	89 \pm 10%
R2B with BAM	30 \pm 6%	70 \pm 6%
MS with BAM	15 \pm 7%	85 \pm 7%

661

Table 4. Stability of the BAM-catabolic genotypes in MSH1-GFP biofilms (Experiment C and D) that developed from the Dcba⁻ or Dcba⁺ MSH1-GFP inoculum when continuously fed with MS medium containing 0, 1, 10, 100 and 1000 µg/L BAM. BAM-degradation efficiency, the total number of MSH1-GFP cells and the MSH1-GFP specific BAM-degradation activity were determined for each condition at the end of the experiment.

BAM feed	<i>bbdA</i> :16S rRNA		<i>bbdD</i> :16S rRNA		BAM-degradation		MSH1-GFP cells ³		Specific degradation	
[µg/L]	gene ratio		gene ratio		efficiency [%]		[cells]		rate ⁴ [µg/cell/min]	
	DCBA ⁻	DCBA ⁺	DCBA ⁻	DCBA ⁺	DCBA ⁻	DCBA ⁺	DCBA ⁻	DCBA ⁺	DCBA ⁻	DCBA ⁺
	Inoculum ¹	Inoculum ²	Inoculum	Inoculum	Inoculum	Inoculum	Inoculum	Inoculum	Inoculum	Inoculum
Inoculum	2.56±0.40	2.40±0.20	0.08±1	2.20±30	-	-	-	-	-	-
-	3.41±0.79	4.64±1.69	0.02±0.00	0.33±0.18	-	-	8.6±1.4 × 10 ⁷	1.2±0.1 × 10 ⁸	-	-
0.9±0.0	4.19±0.20	4.98±0.66	0.03±0.01	0.21±0.08	68±1	77±4	1.6±0.2 × 10 ⁸	1.7±0.3 × 10 ⁸	2.3±0.0 × 10 ⁻¹³	2.5±0.1 × 10 ⁻¹³
6.9±0.0	4.12±0.06	3.11±0.77	0.02±0.01	0.29±0.16	76±4	67±4	2.3±0.2 × 10 ⁸	2.2±0.2 × 10 ⁸	1.4±0.1 × 10 ⁻¹²	1.3±0.1 × 10 ⁻¹²
73.1±0.9	1.93±0.39	1.85±0.78	0.15±0.12	0.18±0.06	83±1	85±2	3.5±0.6 × 10 ⁸	3.2±0.5 × 10 ⁸	1.1±0.0 × 10 ⁻¹¹	1.1±0.0 × 10 ⁻¹¹
733.6±0.9	1.72±1.01	2.58±0.73	0.38±0.11	0.150±0.45	84±1	85±3	5.8±1.2 × 10 ⁸	8.5±1.0 × 10 ⁸	6.4±0.1 × 10 ⁻¹¹	4.4±0.1 × 10 ⁻¹¹
Inoculum	267±33	270±43	3±1	277±21	-	-	-	-	-	-
-	2.47±1.08	3.54±1.21	0.13±0.15	1.90±0.22	-	-	9.1±1.8 × 10 ⁷	9.7±1.3 × 10 ⁷	-	-
1.1±0.0	1.45±0.33	2.18±0.94	0.01±0.02	3.31±0.73	53±2	48±3	9.8±4.2 × 10 ⁷	9.5±2.5 × 10 ⁷	3.3±0.1 × 10 ⁻¹³	3.2±0.2 × 10 ⁻¹³
9.1±0.9	4.90±0.43	2.18±1.77	0.04±0.06	1.66±1.41	35±7	47±9	1.1±0.2 × 10 ⁸	9.3±3.1 × 10 ⁷	1.8±0.4 × 10 ⁻¹²	2.7±0.5 × 10 ⁻¹²
93.5±4.2	3.22±1.63	3.44±0.19	0.17±0.03	1.89±0.85	48±3	57±4	1.1±0.3 × 10 ⁸	1.7±0.2 × 10 ⁸	2.4±0.1 × 10 ⁻¹¹	1.8±0.1 × 10 ⁻¹¹
1102.3±55.0	3.52±0.43	2.46±0.73	1.77±1.06	3.53±1.27	38±0	41±5	2.2±0.6 × 10 ⁸	4.6±1.0 × 10 ⁸	1.1±0.0 × 10 ⁻¹⁰	5.8±0.1 × 10 ⁻¹¹

666 ¹ DCBA⁻ inoculum: MSH1-GFP culture used for inoculation of flow channels was cultivated in R2B with 200 mg/L BAM and has a high incidence of BbdA⁺ Dcba⁻
667 cells.

668 ² DCBA⁺ inoculum: MSH1-GFP culture used for inoculation of flow channels was cultivated in MS with 200 mg/L BAM and has a high incidence of BbdA⁺ Dcba⁺
669 cells.

670 ³ MSH1-GFP cell numbers were calculated by dividing the GFP-labeled biofilm biovolume (μm^3) with the MSH1-GFP cell volume ($0.36 \mu\text{m}^3/\text{cell}$) (10). Values
671 are averages with standard deviation and were derived from nine image stacks (three image stacks taken of each of three biofilms).

672 ⁴ BAM-degradation rate [μg BAM/min] in flow channels were calculated as follows: BAM-degradation efficiency [%] x actual BAM concentration [$\mu\text{g}/\text{L}$] x flow
673 rate [L/min]. Specific BAM-degradation rate [μg BAM/cell/min] was calculated as follows: BAM-degradation rate [μg BAM/min] divided by number of MSH1-
674 GFP cells

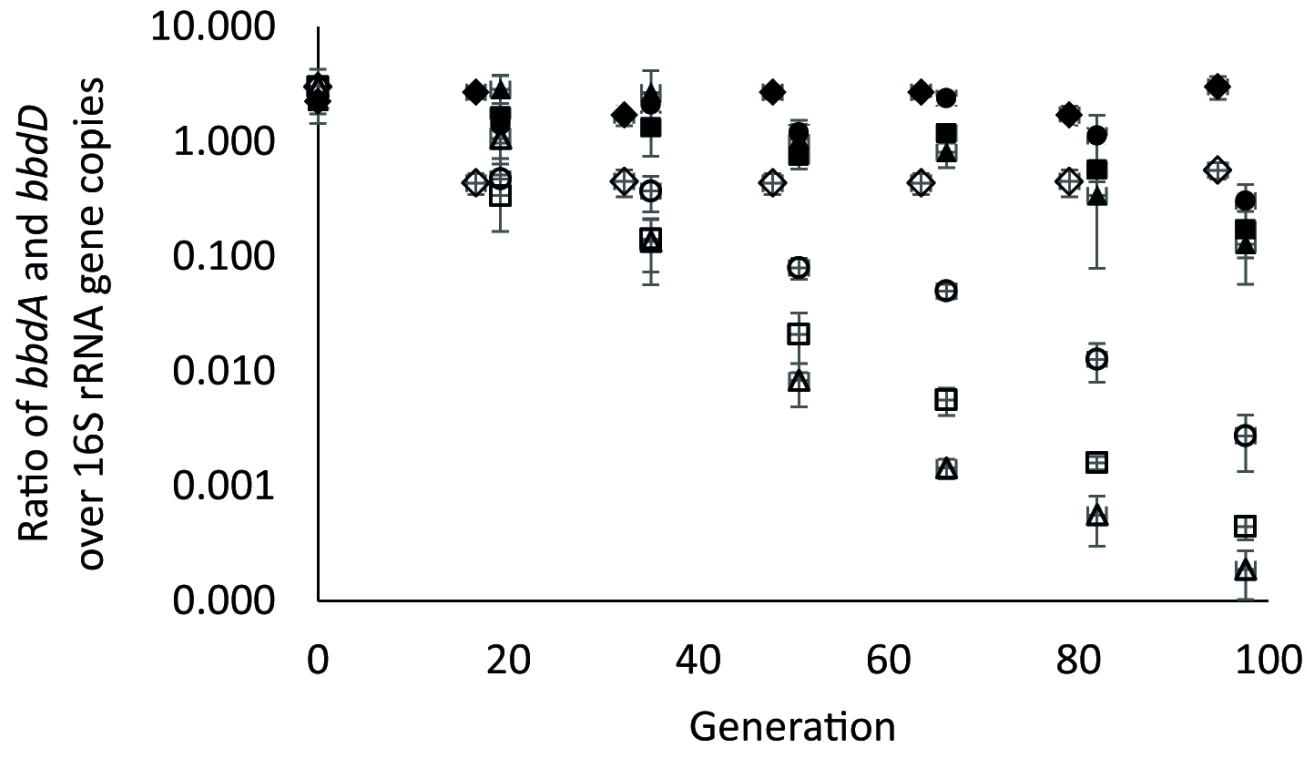
Figure legends

Figure 1. Ratio of *bbdA* (full symbol) and *bbdD* (empty symbol) over 16S rRNA gene copies in function of the generation of MSH1-GFP grown in either R2B (circle), R2B with 20 mg/L BAM (square), R2B with 200 mg/L BAM (triangle) or MS with 200 mg/L BAM (diamond). MSH1-GFP was pre-cultured in MS with 200 mg/L BAM (Experiment B). Values are averages with standard deviation (n=6).

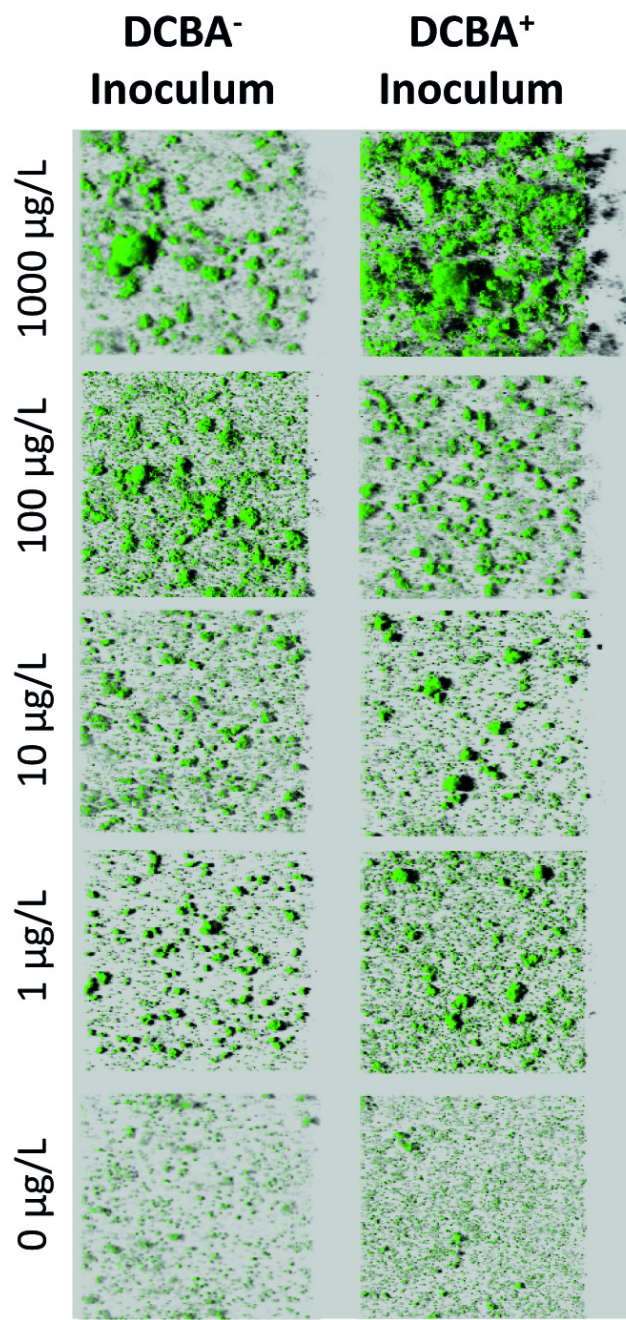
Figure 2. CLSM images of MSH1-GFP biofilms grown in flow channels continuously fed with MS medium containing BAM at 1, 10, 100, 1000 μ g/L and no BAM, without (Experiment C) (left) and with (Experiment D) (right) reduction of AOC in the feed. Biofilms are shown for channels inoculated with an MSH1-GFP inoculum with high incidence of BbdA⁺ Dcba⁻ cells (DCBA⁻) and an inoculum with a high incidence of BbdA⁺ Dcba⁺ cells (DCBA⁺). Biofilm images are top view 3D-representations of image stacks taken with CLSM.

Figure 3. Ratio of *bbdA* (plain bars) and *bbdD* (patterned bars) over 16S rRNA gene copies in the MSH1-GFP culture used for inoculation and in the MSH1-GFP biofilms grown in flow channels fed with MS medium containing no BAM and BAM at 1, 10, 100, 1000 μ g/L without (left panel) (Experiment C) and with (right panel) (Experiment D) reduction of AOC in the feed. Biofilms developed from either a DCBA⁻ (white) and DCBA⁺ (grey) inoculum. Values are averages with standard deviation (n = 6).

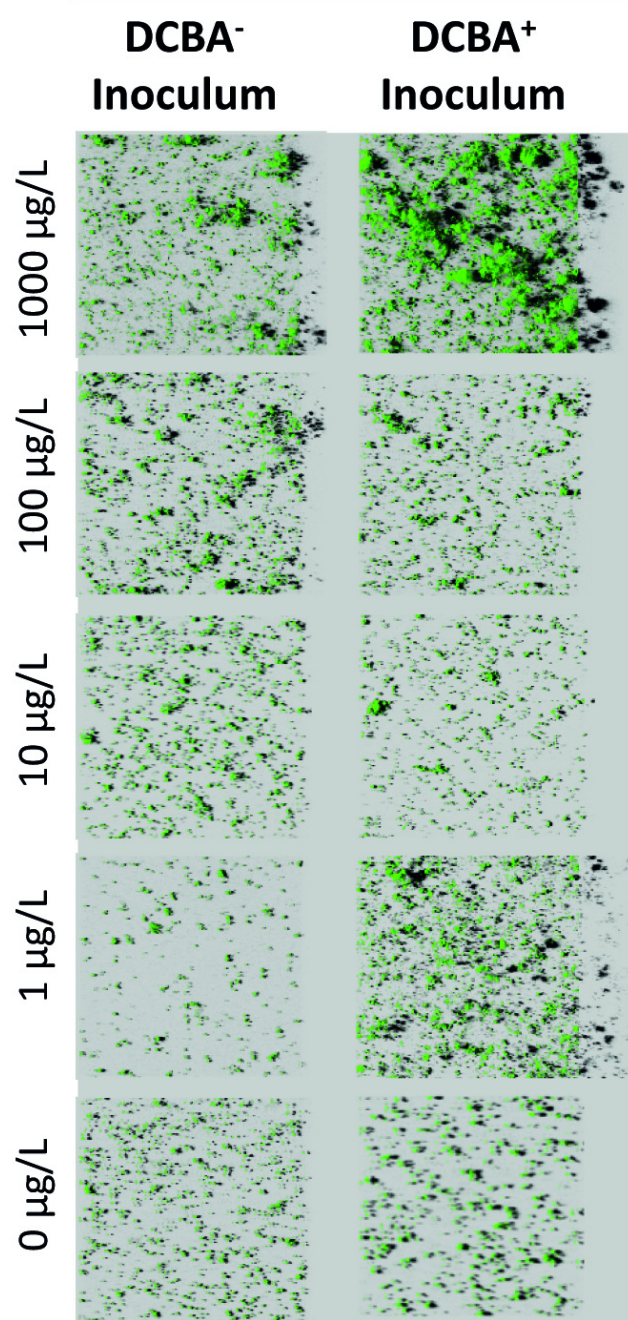
Figure 4. Ratio of *bbdA* (full symbols) and *bbdD* (empty symbols) over 16S rRNA gene copies in top layer (left panel) and effluent (right panel) samples of pilot DWTP sand filters (Experiment E) inoculated with strain MSH1 that treat BAM-contaminated groundwater for drinking water production. The MSH1 inoculum had either a high incidence of BbdA⁺ Dcba⁻ cells (circles) or a high incidence of BbdA⁺ Dcba⁺ cells (squares). Values are averages with standard deviation (n=4).



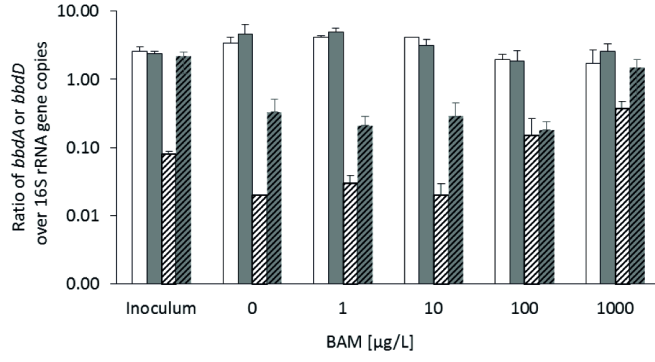
Feed without reduction of AOC



Feed with reduction of AOC



**Feed without
reduction of AOC**



**Feed with
reduction of AOC**

